AGU PUBLICATIONS

Geophysical Research Letters

RESEARCH LETTER
10.1002/2014GL060690

Key Points:
- We detected velocity changes due to the Earth tide from ambient noise analyses
- Ambient noises were examined by applying FK analyses
- The estimated strain sensitivity is consistent with previous results

Supporting Information:
- Readme
- Figure S1
- Figure S2

Correspondence to:
T. Takano,
takano@zisin.gp.tohoku.ac.jp

Citation:
Takano, T., T. Nishimura, H. Nakahara, Y. Ohta, and S. Tanaka (2014), Seismic velocity changes caused by the Earth tide: Ambient noise correlation analyses of small-array data, *Geophys. Res. Lett.*, *41*, 6131–6136, doi:10.1002/2014GL060690.

Received 17 JUN 2014
Accepted 29 JUL 2014
Accepted article online 2 AUG 2014
Published online 11 SEP 2014

Seismic velocity changes caused by the Earth tide: Ambient noise correlation analyses of small-array data

Tomoya Takano[1,2], Takeshi Nishimura[1], Hisashi Nakahara[1], Yusaku Ohta[3], and Sachiko Tanaka[4]

[1]Department of Geophysics, Graduate School of Science, Tohoku University, Sendai, Japan, [2]Now at Japan Radio Co. Ltd., Suginami, Japan, [3]Research Center for Prediction of Earthquakes and Volcanic Eruptions, Graduate School of Science, Tohoku University, Sendai, Japan, [4]National Research Institute for Earth Science and Disaster Prevention, Tsukuba, Japan

Abstract We examine seismic velocity changes due to the Earth tide by conducting cross-correlation function (CCF) analyses of ambient seismic noise recorded at a small array composed of seven seismometers in northeastern Japan. We calculate CCFs for the dilatational and contractional episodes that are predicted from theoretical tidal volumetric strains. CCFs of the two episodes are highly correlated, but tiny differences are found in their phases. The phase differences are explained by seismic velocity changes of $-0.19 \pm 0.06\%$ at 1–2 Hz, which are interpreted to be caused by opening/closure of cracks or pores in the shallow subsurface due to the tidal strain. Strain sensitivities of the seismic velocity changes are estimated to be 6.9×10^4 strain^{-1}, which are almost consistent with those reported in previous studies using artificial sources.

1. Introduction

Seismic velocity changes caused by applied stress or strain are one of the important quantities to characterize the mechanical properties of rocks and shallow structures. Previous studies used the Earth tide as a source of the stress for in situ measurements of the seismic velocity changes [e.g., *De Fazio et al.*, 1973; *Reasenberg and Aki*, 1974; *Yamamura et al.*, 2003]. Measuring the travel times of the seismic waves excited by artificial controlled sources, these previous studies reported seismic velocity changes ranging from 0.1 to 0.5% for the Earth tide at frequencies of tens of hertz to kilohertz.

Temporal changes of the seismic velocity in the crust and shallow subsurface are also detected at the occurrences of large earthquakes or volcanic activities by analyzing repeating earthquakes or artificial sources [e.g., *Poupinet et al.*, 1984; *Nishimura et al.*, 2005]. Recently, temporal changes of structures were widely examined by seismic interferometry using cross-correlation functions (CCFs) of ambient noise at two stations [e.g., *Wegler et al.*, 2009; *Anggono et al.*, 2012], because retrieved CCFs are equivalent to Green's function between the two stations [e.g., *Snieder*, 2004].

In this study, we investigate seismic velocity changes due to the Earth tide in shallow structure by applying coda wave interferometry to ambient noise CCFs. We estimate the strain sensitivity of seismic velocity changes in a frequency band of 1–2 Hz. In the process, we examine the distribution of the ambient noise using seismic array analyses to aid our understanding the mechanism of seismic velocity changes detected in this study.

2. Data

We deployed a small triangle-shaped array consisting of seven seismometers at the east foot of Iwate volcano in northeastern Japan, for approximately 3 months : 1 December 2012 to 26 February 2013 (Figure 1). We installed six short-period vertical component seismometers (natural frequency $f_0 = 2$ Hz, L-22D, Sercel Co.) and a three-component seismometer ($f_0 = 2$ Hz, KVS-300, Kinkei system Co.). These seismometers were moving-coil sensors and were placed at apices of a triangle with an average side length of 200 m. We placed the other four sensors at the middle point of each side of the triangle and at the center. Each sensor was buried at a depth of approximately 0.5 m. The seismic signals were recorded by data loggers (EDR-X7000, Kinkei system Co.) with a sampling frequency of 1 kHz and an analog to digital resolution of 18 bits. The internal clock of the data loggers was corrected by a GPS clock whose error is less than 1 ms. The frequency band of 1–2 Hz we analyze is close to or less than the natural frequency of seismometers; therefore, small differences in the natural frequencies of the seismometers may introduce phase differences. Hence, we

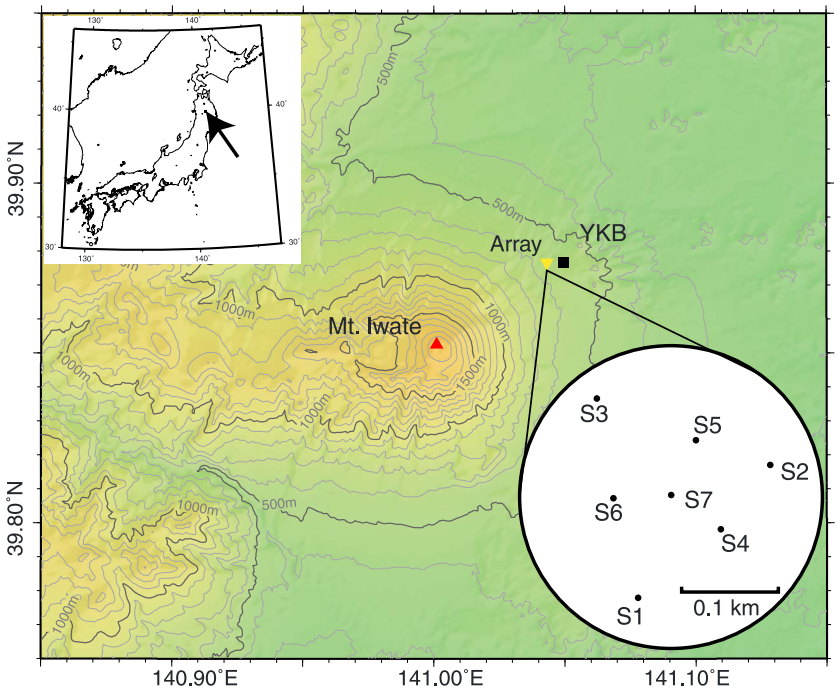

Figure 1. Location of the seismic array on the foot of Mount Iwate. Small array (triangle); YKB station (square). Three-component seismometer is set at S1.

examine azimuths of *P* wave from regional earthquakes with frequency-wave number (FK) analyses and confirm that the obtained azimuths matched well with those calculated from the epicenters determined by the Japanese network stations. Moreover, we mainly examine temporal changes of the seismic velocity. Therefore, no instrumental correction is done in the following analyses.

3. Method

To examine temporal changes of the shallow subsurface due to the Earth tide, we divide the observation period into two episodes: dilatational and contractional, according to tidal volumetric strain values. The volumetric strain due to the Earth tide at the array location is calculated using GOTIC2 program [*Matsumoto et al.*, 2001], which includes the effect of oceanic loading in the calculation with an ocean tide model based on TOPEX/POSEIDON data. Amplitudes of the tidal strain vary from -2×10^{-8} to 3×10^{-8} with the dominant period of 12.42 h of M2 component (semidiurnal tides caused by the Moon) during the observation periods (Figure S1 in the supporting information). We define the dilatational and contractional episodes to be the periods with strain amplitudes of more than 5×10^{-9} and those of less than -5×10^{-9}, respectively. We confirm that the volumetric strain calculated with GOTIC2 is in phase with the records of a borehole strain meter located at a depth of 300 m at YKB station of Tohoku University, which is located 0.5 km away from the array [*Sato and Hamaguchi*, 2006]. In the following analyses, we use the theoretical strains by GOTIC2, because the observed strains contain long-period noises that are probably caused by rainfalls, ground water changes, and unknown sources. Figure 2 shows the total data length of the dilatational and contractional periods for each hour of the day during our observation period for the 3 months. Most of the data in the dilatational episode are distributed in the morning of local time, while the data in the contractional episode appear at night. These differences of time zones among the two episodes may affect the noise distributions and CCFs. Hence, we select the ambient noise observed in a time zone of 2 h–4 h when the recording durations are nearly same for the two episodes. The total time of the data in the dilatational episode we analyze is 6171 min, while that of the contractional episode is 4755 min.

We calculate CCF for each pair selected from the stations numbered S1 to S7 (Figure 1). The seismic data are first filtered at 1–2 Hz. We use the data with amplitudes less than 5 times of the RMS amplitude of

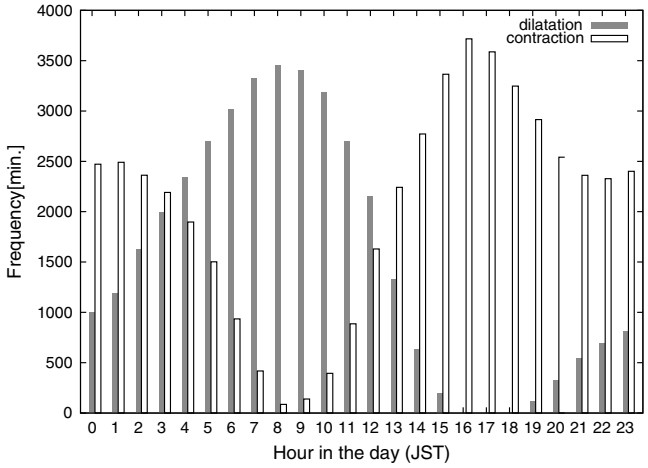

Figure 2. Frequency of dilatational episodes (grey) and contractional episodes (white) during our observation period.

averaged noise signals to avoid earthquake signals and large unknown noise. We apply 1 bit normalization to enhance phase information in the ambient noise [*Bensen et al.*, 2007]. CCFs are calculated every minute and separately stacked for the dilatational episode and the contractional one in 2 h–4 h to obtain CCF for the dilatational episode (hereafter called DCCF) and that for the contractional episode (CCCF). We compare DCCF and CCCF to estimate seismic velocity changes due to the Earth tide. Because the seismic array size is comparable to the wavelength of ambient noise, auto-correlation function (ACF) calculated at each station is similar in shape with waveforms in negative or positive lag times of CCFs. ACFs may also be used for the following analyses. But, in the present study, we examine CCFs because time differences in both of negative and positive lag times are measurable.

4. Results

Figure 3 shows DCCF and CCCF at 1–2 Hz for the station pair of S3 and S7. We calculate correlation coefficients and time differences using cross correlation between DCCF and CCCF. Because DCCF is highly correlated with CCCF, we shift a time window of 1.024 s every 0.256 s to detect small differences in cross-correlation functions. The correlation coefficients of DCCF and CCCF are estimated to be more than 0.99 (Figure 3). Closely looking at the CCFs, we find that peaks of DCCFs are slightly delayed to those of CCCFs at lag times, τ, of about ±0.6 s. Time differences at negative and positive lag times are almost symmetric with respect to $\tau = 0$ s. This suggests that the change is caused by seismic velocity changes of the medium around the stations rather than changes of noise source locations [*Stehly et al.*, 2006].

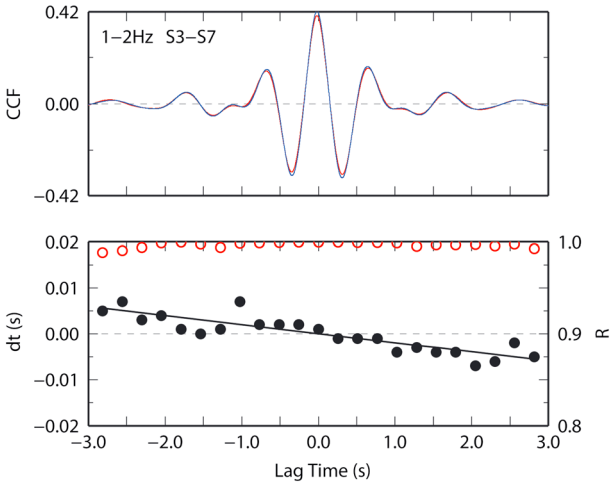

Figure 3. Comparison of DCCF to CCCF at a frequency band of 1–2 Hz for the station pair of S3 and S7. (top) Red and blue lines indicate DCCF and CCCF, respectively. (bottom) Red open circles indicate correlation coefficients (*R*), and black dots represent time differences (d*t*) between DCCF and CCCF. Solid line indicates the best fitted line to the time differences.

The other 20 station pairs also show the same characteristics in DCCFs and CCCFs. To determine an average characteristic of the changes, we stack the correlation coefficients and time differences of all pairs (Figure 4). Averages of the correlation coefficients are higher than 0.99 at lag times of −3 s to +3 s, and the averaged time difference changes almost linearly at lag times from −3 s to +3 s. However, we see a small degradation of correlation coefficients at lag times of $\tau = -3$ s and $\tau = 3$ s. Furthermore, linearity of time differences is not well recognized at $|\tau| > 3$ s. This is not caused by cycle skipping due to a short time window (1.024 s), and we discuss this characteristic in relation to the wave properties of the ambient noise in the next section. In the following analyses, we only consider CCFs with the lag times from −3 s to +3 s.

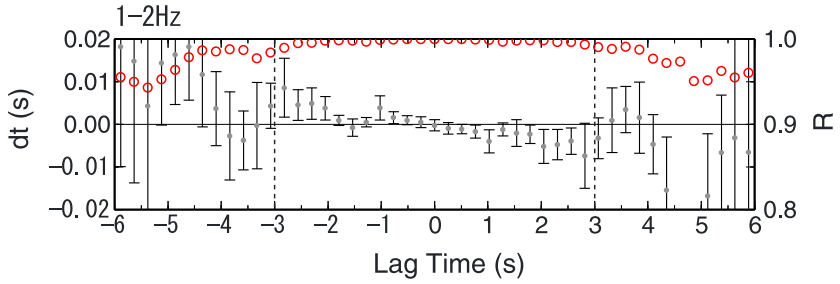

Figure 4. Time differences and correlation coefficients averaged for the results from all station pairs. Grey solid circles with error bars denote time differences, and correlation coefficients are denoted by red open circles. Broken lines at ±3 s indicate lag time ranges where we estimate the velocity changes.

Assuming a homogeneous medium around the stations, we estimate seismic velocity changes using a relation of $dv/v = -d\tau/\tau$, where v is the seismic velocity [*Poupinet et al.*, 1984]. Based on the calculated time differences, we estimate velocity changes for all 21 pairs of stations.

Figure 5 shows the estimated seismic velocity changes for each station pair. We recognize seismic velocity decreases of about 0.1–0.3% during the dilatational episode with respect to the contractional episode. We do not find significant azimuthal dependence of the seismic velocity changes. Station pairs including S7 tend to show larger velocity changes. This may be related to small-scale structural changes beneath the array. The averages and standard deviations of the seismic velocity changes are estimated to be −0.19% and 0.06%, respectively, for the 21 pairs. We further estimate strain sensitivities of the seismic velocity changes (i.e., $dv/v(d\epsilon)^{-1}$, where ϵ represents the strain) to be 6.9×10^4 strain^{-1} from the average seismic velocity changes and the average volumetric strain changes (2.6×10^{-8}) during the dilatational and contractional episodes.

It is difficult to estimate the steady velocity changes at higher frequency bands (2–8 Hz) because of low correlations between DCCFs and CCCFs. We also compare DCCFs and CCCFs from all of the data recorded during our observation (i.e., 0–23 h). The results show similar time differences between DCCFs and CCCFs. Even for a higher frequency band (2–4 Hz) and a wider frequency band (1–8 Hz), we see time differences that are explained by the seismic velocity changes around the stations. Because the cross-correlation coefficients between DCCFs and CCCFs for the all data (0–23 h) are less than those for the limited data from 2 h to 4 h, we use the result of the latter.

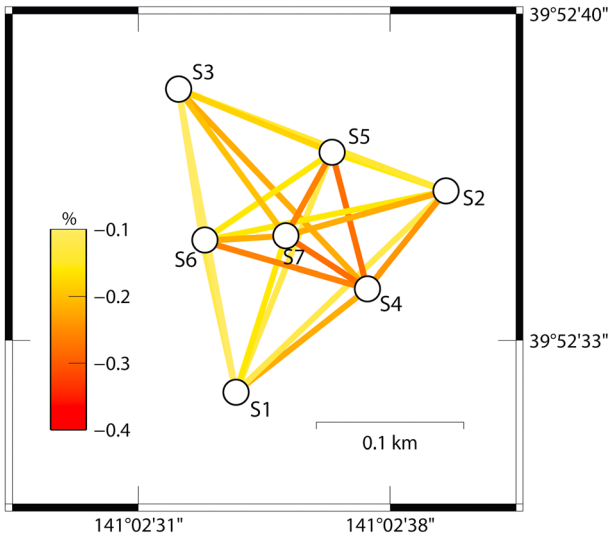

Figure 5. Seismic velocity decreases of DCCF with respect to CCCF at the array. Colors of lines connecting two stations represent the velocity changes detected from analyses of the two stations.

5. Discussion

Opening and closing of cracks or pores in rock according to the changes in confining pressure make the seismic velocity decrease and increase, respectively. The observed seismic velocity decreases during the dilatational episode with respect to the contractional episode are consistent with this mechanism. Thus, we conclude that the strain by the Earth tide causes the seismic velocity changes at shallow depths beneath the seismic array.

The stress sensitivities of the seismic velocity changes, instead of the strain sensitivity, are estimated in previous studies [*De Fazio et al.*, 1973; *Reasenberg*

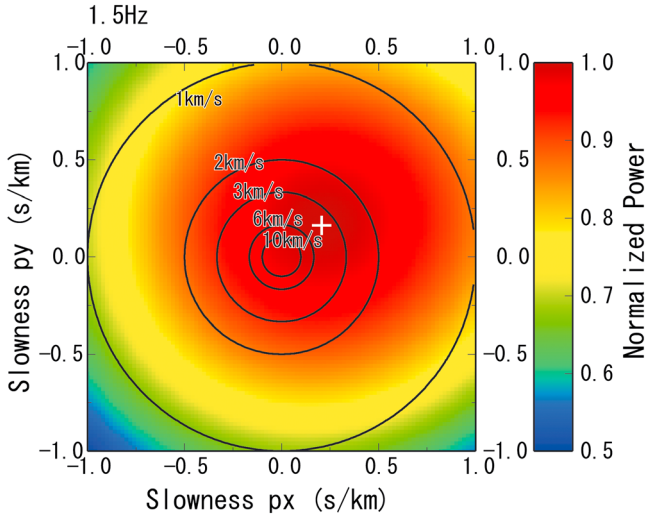

Figure 6. FK spectrum at dominant frequencies of 1.5 Hz in the observation periods. A white cross in the panel shows a peak value of normalized power. Circles are drawn for the apparent velocities of 10 km/s, 6 km/s, 3 km/s, 2 km/s, and 1 km/s.

and Aki, 1974; *Yamamura et al*., 2003]. *De Fazio et al*. [1973] conducted an experiment along a mine shaft composed of calcite at a shallow depth (37–173 m) using a 500 Hz hydraulic vibrator; *Reasenberg and Aki* [1974] used an air gun as a seismic source on exposed granite rock over a distance of 200 m; *Yamamura et al*. [2003] conducted 1 year continuous measurements using a piezoelectric transducer across a distance of 12 m in a vault composed of andesitic clay-rich lapilli tuff. As summarized in Table 1 of *Yamamura et al*. [2003], these experiments show the stress sensitivities of the seismic velocity changes ranging from 0.5×10^{-7} to 2×10^{-6} Pa^{-1}. These values obtained at high frequency ranges are less than or almost equal to our result at 1–2 Hz within a factor of about 2, because the strain sensitivity (6.9×10^{4} strain^{-1}) is equivalent to 3.5×10^{-6} Pa^{-1} for the medium with a bulk modulus of 2×10^{10} Pa.

It is necessary to know the characteristics of the ambient noise in order to understand the wave types composing DCCFs and CCCFs and interpret the observed time differences between them. We apply frequency-wave number (FK) analysis to the ambient noise recorded at the array and calculate a cross spectrum for a time window of 8.192 s with a 5% cosine taper, averaging over nine discrete frequencies. We normalize the cross spectrum by the power spectrum and stack them for the entire observation period to obtain an averaged FK spectrum. Figure 6 shows the averaged FK spectra at 1.5 Hz in the two-dimensional slowness domain. The peak of the power is located at a slowness of 0.28 s/km. Large powers of more than 0.8 spread over a large area of the slowness domain. But the width of the observed power spectrum is about 25% wider than that of the array response; hence, we may roughly estimate that the slowness of the ambient noise distributes in the range of 0.35–0.21 s/km. The first arrival times obtained by an active seismic experiment of the volcanic structure at Mount Iwate [*Tanaka et al*., 2002] indicates *P* wave velocity of about 3 km/s around the array. Hence, the ambient noise contains both body waves and surface waves, although it is difficult to determine the ratio of wave type energy.

In our study, we found the linearity of the time difference at lag times between −3 s and +3 s, but not in the later parts of CCFs at small (< −3 s) or large (> +3 s) lag times (Figure 4). Because the waveforms of CCFs in negative and positive lag times resemble auto-correlation functions at each seismometer, the CCFs at small and large lag times can be interpreted as the body and/or surface waves reflecting from shallow medium around the array and those propagating long distances, respectively. At lag times between −3 s and 3 s, therefore, the CCFs come to consist of body waves and surface waves propagating in shallow subsurface with a depth of less than a few kilometers, where the confining pressure is small so that the tidal stress can change the seismic velocity. On the other hand, the later part of CCFs, which do not show linearity in the time differences, are considered to mainly consist of body waves propagating in deep regions where tidal effects on the seismic velocity are small. This is because if surface waves were dominant, linearity of the time difference are expected to be also detected in the later parts of CCFs. But this is not consistent with our observation, as the time differences at lag times from −4 to −3 s and from 3 to 4 s are estimated to be around zero. This interpretation also matches with recent numerical simulation results by *Obermann et al*. [2013] that show the importance of body wave for the sensitivity of coda waves at deep depths in late coda. At lag times, less than −4 s and larger than 4 s polarities of the time differences are matched with the predictions from the tidal effect. However, we may not discuss them in detail because the estimation errors are large and Green's function may not be fully converged.

6. Conclusions

We have detected seismic velocity changes that are interpreted to be caused by opening/closure of cracks or pores in the shallow subsurface due to the Earth tide from coda wave interferometry analyses of ambient noise CCFs recorded at a small seismic array in northeastern Japan. Seismic velocity changes of DCCF with respect to CCCF are estimated to be $-0.19 \pm 0.06\%$ at 1–2 Hz. The estimated strain sensitivity of the seismic velocity changes of 6.9×10^4 strain^{-1} is consistent with the sensitivities at higher frequencies that were reported in previous active experimental studies.

Since the Earth tide is ubiquitous and seismic interferometry can be applied in any place where seismometers are installed, our approach may provide a way to measure a property of rocks and shallow structure in situ. These measurements of the Earth tide response from ambient seismic noise may also be useful to quantitatively discuss observed seismic velocity changes associated with coseismic displacement or volcanic crustal deformation [e.g., *Anggono et al.*, 2012; *Nishimura et al.*, 2005] and to understand the strain rate dependency of the seismic velocity changes in the crustal structure [*Rivet et al.*, 2011].

Acknowledgments

We are grateful that Iwate Yakebashiri International Exchange Village allowed us to deploy a seismic array. Thoughtful comments of Dylan Mikesell and an anonymous reviewer improved the manuscript. We thank Michael Wysession for his editorial efforts. This study is partly supported by JSPS KAKENHI grant 24654141.

The Editor thanks Thomas Mikesell and an anonymous reviewer for their assistance in evaluating this paper.

References

Anggono, T., T. Nishimura, H. Sato, H. Ueda, and M. Ukawa (2012), Spatio-temporal changes in seismic velocity associated with the 2000 activity of Miyakejima volcano as inferred from cross-correlation analyses of ambient noise, *J. Volcanol. Geotherm. Res.*, *247–248*, 93–107.

Bensen, G. D., M. H. Ritzwoller, M. P. Barmin, A. L. Levshin, F. Lin, M. P. Moschetti, N. M. Shapiro, and Y. Yang (2007), Processing seismic ambient noise data to obtain reliable broad-band surface wave dispersion measurements, *Geophys. J. Int.*, *169*, 1239–1260, doi:10.1111/j.1365-246X.2007.03374.x.

De Fazio, T. L., K. Aki, and J. Alba (1973), Solid earth tide and observed change in the in situ seismic velocity, *J. Geophys. Res.*, *78*, 1319–1322, doi:10.1029/JB078i008p01319.

Matsumoto, K., K. Sato, T. Takanezawa, and M. Ooe (2001), GOTIC2: A program for computation of oceanic tidal loading effect, *J. Geod. Soc. Jpn.*, *47*, 243–248.

Nishimura, T., S. Tanaka, T. Yamawaki, H. Yamamoto, T. Sano, M. Sato, H. Nakahara, N. Uchida, S. Hori, and H. Sato (2005), Temporal changes in seismic velocity of the crust around Iwate volcano, Japan, as inferred from analyses of repeated active seismic experiment data from 1998 to 2003, *Earth Planets Space*, *57*, 491–505.

Obermann, A., T. Planès, E. Larose, C. Sens-Schönfelder, and M. Campillo (2013), Depth sensitivity of seismic coda waves to velocity perturbations in an elastic heterogeneous medium, *Geophys. J. Int.*, *194*(1), 372–382, doi:10.1093/gji/ggt043.

Poupinet, G., W. L. Ellsworth, and J. Frechet (1984), Monitoring velocity variations in the crust using earthquake doublets: An application to the Calaveras fault, California, *J. Geophys. Res.*, *89*, 5719–5731, doi:10.1029/JB089iB07p05719.

Reasenberg, P., and K. Aki (1974), A precise, continuous measurement of seismic velocity for monitoring in situ stress, *J. Geophys. Res.*, *79*(2), 399–406, doi:10.1029/JB079i002p00399.

Rivet, D., M. Campillo, N. M. Shapiro, V. Cruz-Atienza, M. Radiguet, N. Cotte, and V. Kostoglodov (2011), Seismic evidence of nonlinear crustal deformation during a large slow slip event in Mexico, *Geophys. Res. Lett.*, *38*, L08308, doi:10.1029/2011GL047151.

Sato, M., and H. Hamaguchi (2006), Weak long-lived ground deformation related to Iwate volcanism revealed by Bayesian decomposition of strain, tilt and positioning data, *J. Volcanol. Geotherm. Res.*, *155*, 244–262.

Snieder, R. (2004), Extracting the Green's function from the correlation of coda waves: A derivation based on stationary phase, *Phys. Rev. E*, *69*, 046610, doi:10.1103/PhysRevE.69.046610.

Stehly, L., M. Campillo, and N. M. Shapiro (2006), A study of the seismic noise from its long-range correlation properties, *J. Geophys. Res.*, *111*, B10306, doi:10.1029/2005JB004237.

Tanaka, S., et al. (2002), Seismic exploration at Iwate volcano with active sources—The outline of the experiment and the first arrival time data [in Japanese with English abstract], *Bull. Earthquake Res. Inst.*, *77*, 1–25.

Wegler, U., H. Nakahara, C. Sens-Schonfelder, M. Korn, and K. Shiomi (2009), Sudden drop of seismic velocity after the 2004 *Mw* 6.6 mid-Niigata earthquake, Japan, observed with passive image interferometry, *J. Geophys. Res.*, *114*, B06305, doi:10.1029/2008JB005869.

Yamamura, K., O. Sano, H. Utada, Y. Takei, S. Nakao, and Y. Fukao (2003), Long-term observation of in situ seismic velocity and attenuation, *J. Geophys. Res.*, *108*(B6), 2317, doi:10.1029/2002JB002005.